

**MIXED CONVECTIVE HEAT AND MASS TRANSFER FLOW OF A VISCOUS FLUID  
IN A VERTICAL CHANNEL WITH THERMAL RADIATION AND SORLET EFFECT**

**Siva Gopal R\*<sup>1</sup>, U. Rajeswara Rao<sup>1</sup> and D.R.V. Prasada Rao<sup>1</sup>**

*<sup>1</sup>Department of Mathematics, S.K. University, Anantapur, A.P, India.*

*(Received on: 08-03-14; Revised & Accepted on: 21-03-14)*

---

**ABSTRACT**

*We made an attempt in this dissipation study effect of radiation and thermo-diffusion on non-Darcy convective heat and mass transfer flow of a viscous, electrically conducting fluid through a porous medium in a vertical channel in the presence of heat generating sources. The governing equations flow, heat and mass transfer are solved by using regular perturbation method with  $\delta$ , the porosity parameter as a perturbation parameter. The velocity, temperature, concentration, shear stress and rate of Heat and Mass transfer on the walls are evaluated numerically for different variations of parameter.*

**Key Words:** *Heat and Mass Transfer, Viscous Fluid, Vertical Channel, Thermal Radiation and Soret Effect.*

---

**1. INTRODUCTION**

The phenomenon of heat and mass transfer has been the object of extensive research due to its applications in Science and Technology. Such phenomena are observed in buoyancy induced motions in the atmosphere, in bodies of water, quasisolid bodies such as earth and so on.

Non-Darcy effects on natural convection in porous media have received a great deal of attention in recent years because of the experiments conducted with several combinations of solids and fluids covering wide ranges of governing parameters which indicate that the experimental data for systems other than glass water at low Rayleigh numbers, do not agree with theoretical predictions based on the Darcy flow model. This divergence in the heat transfer results has been reviewed in detail in Cheng (7) and Prasad *et al.* (15) among others. Extensive effects are thus being made to include the inertia and viscous diffusion terms in the flow equations and to examine their effects in order to develop a reasonable accurate mathematical model for convective transport in porous media. The work of Vafai and Tien (21) was one of the early attempts to account for the boundary and inertia effects in the momentum equation for a porous medium. They found that the momentum boundary layer thickness is of order of  $\sqrt{\frac{k}{\epsilon}}$ . Vafai and Thiyagaraja (22) presented analytical solutions for the velocity and temperature fields for the interface region using the Brinkman Forchheimer – extended Darcy equation. Detailed accounts of the recent efforts on non-Darcy convection have been recently reported in Tien and Hong (19), Cheng (7), Prasad *et al.* (17), and Kladias and Prasad (11). Here, we will restrict our discussion to the vertical cavity only. Poulidakos and Bejan (14) investigated the inertia effects through the inclusion of Forchheimer's velocity squared term, and presented the boundary layer analysis for tall cavities. They also obtained numerical results for a few cases in order to verify the accuracy of their boundary layer analysis for tall cavities. They also obtained numerical results for a few cases in order to verify the accuracy of their boundary layer solutions. Later, Prasad and Tuntomo (15) reported an extensive numerical work for a wide range of parameters, and demonstrated that effects of Prandtl number remain almost unaltered while the dependence on the modified Grashof number, Gr, changes significantly with an increase in the Forchheimer number. This result in reversal of flow regimes from boundary layer to asymptotic to conduction as the contribution of the inertia term increases in comparison with that of the boundary term. They also reported a criterion for the Darcy flow limit.

---

**Corresponding author: Siva Gopal R\*<sup>1</sup>**

**<sup>1</sup>Department of Mathematics, S.K. University, Anantapur, A.P, India.**

**E-mail: [sivagopal222@gmail.com](mailto:sivagopal222@gmail.com)**

The Brinkman – Extended – Darcy modal was considered in Tong and Subramanian (20), and Lauriat and Prasad (23) to examine the boundary effects on free convection in a vertical cavity. While Tong and Subramanian performed a Weber – type boundary layer analysis, Lauriat and Prasad (23) solved the problem numerically for A=1 and it was shown that for a fixed modified Rayleigh number, Ra, the Nusselt number; decrease with an increase in the Darcy number; the reduction being larger at higher values of Ra. A scale analysis as well as the computational data also showed that the transport term  $(\mathbf{v} \cdot \nabla) \mathbf{v}$ , is of low order of magnitude compared to the diffusion plus buoyancy terms. A numerical study based on the Forchheimer-Brinkman-Extended Darcy equation of motion has also been reported recently by Beckerman *et al* (4). They demonstrated that the inclusion of both the inertia and boundary effects is important for convection in a rectangular packed – sphere cavity.

Also in all the above studies the thermal diffusion effect (known as Soret effect) has been neglected. This assumption is true when the concentration level is very low. There are some exceptions, the thermal diffusion effects for instance, has been utilized for isotropic separation and in mixtures between gases with very light molecular weight (H<sub>2</sub>, He) and the medium molecular weight (N<sub>2</sub>, air) the diffusion – thermo effects was found to be of a magnitude just it can not be neglected. In view of the importance of this diffusion – thermo effect, recently Jha and Singh (9) studied the free convection and mass transfer flow in an infinite vertical plate moving impulsively in its own plane taking into account the Soret effect. Kafousias (10) studied the MHD free convection and mass transfer flow taking into account Soret effect. The analytical studies of Jha and Singh and Kafousias (9, 10) were based on Laplace transform technique. Abdul Sattar and Alam (1) have considered an unsteady convection and mass transfer flow of viscous incompressible and electrically conducting fluid past a moving infinite vertical porous plate taking into the thermal diffusion effects. Similarity equations of the momentum energy and concentration equations are derived by introducing a time dependent length scale. Malsetty *et al* (12) have studied the effect of both the soret coefficient and Dufour coefficient on the double diffusive convective with compensating horizontal thermal and solutal gradients. Bharathi (5) has studied thermo-diffusion effect on unsteady convective Heat and Mass transfer flow of a viscous fluid through a porous medium in vertical channel. Balasubramanyam *et al* (3) have discussed non-darcy viscous electrically conducting heat and mass transfer flow through a porous medium in a vertical channel in the presence of heat generating sources. Devika Rani *et al* (8) is analysed the effect of radiation on non-darcy convective heat transfer through a porous medium in a vertical channel. Chamkha *et al* (6) studied unsteady natural convective power-law fluid flow past a vertical plate embedded in a non-Darcian porous medium in the presence of a homogeneous chemical reaction. Rashad *et al* (18) have studied in MHD effects on non-Darcy forced convection boundary layer flow past a permeable wedge in a porous medium with uniform heat flux.

Keeping the above application in view we made an attempt in this dissipation study effect of radiation and thermo-diffusion on non-Darcy convective heat and mass transfer flow of a viscous, electrically conducting fluid through a porous medium in a vertical channel in the presence of heat generating sources. The governing equations flow, heat and mass transfer are solved by using regular perturbation method with  $\delta$ , the porosity parameter as a perturbation parameter. The velocity, temperature, concentration, shear stress and rate of Heat and Mass transfer on the walls are evaluated numerically for different variations of parameter.

## 2. FORMULATION OF THE PROBLEM

We consider a fully developed laminar convective heat and mass transfer flow of a viscous, electrically conducting fluid through a porous medium confined in a vertical channel bounded by flat walls. We choose a Cartesian co-ordinate system O(x,y,z) with x- axis in the vertical direction and y-axis normal to the walls the walls are taken at  $y = \pm L$ . The walls are maintained at constant temperature and concentration. The temperature gradient in the flow field is sufficient to cause natural convection in the flow field .A constant axial pressure gradient is also imposed so that this resultant flow is a mixed convection flow. The porous medium is assumed to be isotropic and homogeneous with constant porosity and effective thermal diffusivity. The thermo physical properties of porous matrix are also assumed to be constant and Boussineq’s approximation is invoked by confining the density variation to the buoyancy term. In the absence of any extraneous force flow is unidirectional along the x-axis which is assumed to be infinite.

The Brinkman-Forchheimer-extended Darcy equation which account for boundary inertia effects in the momentum equation is used to obtain the velocity field. Based on the above assumptions the governing equations in the vector form are

$$\nabla \cdot \bar{q} = 0 \quad (\text{Equation of continuity}) \tag{1}$$

$$\frac{\rho}{\delta} \frac{\partial \bar{q}}{\partial t} + \frac{\rho}{\delta^2} (\bar{q} \cdot \nabla) \bar{q} = -\nabla p + \rho g - \left(\frac{\mu}{k}\right) \bar{q} - \mu_e (\bar{J} \times \bar{H}) - \frac{\rho F}{\sqrt{k}} \bar{q} \cdot \bar{q} + \mu \nabla^2 \bar{q} \tag{2}$$

(Equation of linear momentum)

$$\rho C_p \left( \frac{\partial T}{\partial t} + (\bar{q} \cdot \nabla) T \right) = \lambda \nabla^2 T + Q(T_o - T) \tag{3}$$

(Equation of energy)

$$\frac{\partial C}{\partial t} + (\bar{q} \cdot \nabla) C = D_1 \nabla^2 C + k_{11} \nabla^2 T \tag{4}$$

(Equation of diffusion)

$$\rho - \rho_0 = -\beta \rho_0 (T - T_0) - \beta^* \rho_0 (C - C_0) \tag{5}$$

(Equation of State)

Ohm's law

$$\bar{J} = \sigma (\bar{E} + \mu_e \bar{q} \times \bar{H}) \tag{6}$$

where  $\bar{q} = (u, 0, 0)$  is the velocity, T, C are the temperature and Concentration, p is the pressure,  $\rho$  is the density of the fluid,  $C_p$  is the specific heat at constant pressure,  $\mu$  is the coefficient of viscosity, k is the permeability of the porous medium,  $\delta$  is the porosity of the medium,  $\beta$  is the coefficient of thermal expansion,  $\lambda$  is the coefficient of thermal conductivity, F is a function that depends on the Reynolds number and the microstructure of porous medium,  $\beta^*$  is the volumetric coefficient of expansion with mass fraction concentration, k is the chemical reaction coefficient and  $D_1$  is the chemical molecular diffusivity,  $k_{11}$  is the cross diffusivity and Q is the strength of the heat generating source. Here, the thermophysical properties of the solid and fluid have been assumed to be constant except for the density variation in the body force term (Boussinesq approximation) and the solid particles and the fluid are considered to be in the thermal equilibrium). J is the current density,  $\sigma$  is the electrical conductivity of the fluid,  $\bar{E}$  is the applied electric field,  $\mu_e$  is the magnetic permeability,  $\bar{H}$  is the magnetic field vector.

Since the flow is unidirectional, the continuity of equation (1) reduces to

$$\frac{\partial u}{\partial x} = 0 \quad \text{Where } u \text{ is the axial velocity implies } u = u(y)$$

The momentum, energy and diffusion equations in the scalar form reduces to

$$-\frac{\partial p}{\partial x} + \left( \frac{\mu}{\delta} \right) \frac{\partial^2 u}{\partial y^2} - \left( \frac{\mu}{k} \right) u - \left( \frac{\sigma \mu_e^2 H_o^2}{\rho_0} \right) u - \frac{\rho \delta F}{\sqrt{k}} u^2 - \rho g = 0 \tag{7}$$

$$\rho_0 C_p u \frac{\partial T}{\partial x} = \lambda \frac{\partial^2 T}{\partial y^2} + Q(T_o - T) - \frac{\partial(q_R)}{\partial y} \tag{8}$$

$$u \frac{\partial C}{\partial x} = D_1 \frac{\partial^2 C}{\partial y^2} + k_{11} \frac{\partial^2 T}{\partial y^2} \tag{9}$$

The boundary conditions are

$$\begin{aligned} u = 0, \quad T = T_1 \quad C = C_1 \quad \text{on} \quad y = -L \\ u = 0, \quad T = T_2 \quad C = C_2 \quad \text{on} \quad y = +L \end{aligned} \tag{10}$$

The axial temperature and concentration gradients  $\frac{\partial T}{\partial x}$  &  $\frac{\partial C}{\partial x}$  are assumed to be constant, say, A & B respectively.

Using Roseland approximation the Radiative heat flux is given by

$$q_r = -\frac{4\sigma^*}{3\beta_r} \frac{\partial(T'^4)}{\partial y}$$

And expanding  $T'^4$  about  $T_e$  by Taylor's theorem

$$\text{We get } T'^4 \approx 4T_e^3 T - 3T_e^4$$

We define the following non-dimensional variables as

$$u' = \frac{u}{(v/L)}, (x', y') = (x, y)/L, p' = \frac{p\delta}{(\rho v^2/L^2)} \tag{11}$$

$$\theta = \frac{T-T_2}{T_1-T_2}, C' = \frac{C-C_2}{C_1-C_2}$$

Introducing these non-dimensional variables the governing equations in the dimensionless form reduce to (on dropping the dashes)

$$\frac{d^2u}{dy^2} = \pi + \delta(D^{-1} + M^2)u - \delta^2\Delta u^2 - \delta G(\theta + NC) \tag{12}$$

$$\left(1 + \frac{4}{3N_1}\right) \frac{d^2\theta}{dy^2} - \alpha\theta = (PN_T)u \tag{13}$$

$$\frac{d^2C}{dy^2} = (Sc N_c)u + \frac{ScS_0}{N} \frac{d^2\theta}{dy^2} \tag{14}$$

where  $\Delta = FD^{-1/2}$  (Inertia or Fochhemeir parameter)  $G = \frac{\beta g(T_1 - T_2)L^3}{v^2}$  (Grashof Number)

$M^2 = \frac{\sigma\mu_e^2 H_o^2 L^2}{v^2}$  (Hartmann Number),  $D^{-1} = \frac{L^2}{k}$  (Darcy parameter)

$Sc = \frac{v}{D_1}$  (Schmidt number),  $S_0 = \frac{k_{11}\beta^*}{v\beta}$  (Soret parameter)

$N = \frac{\beta^*(C_1 - C_2)}{\beta(T_1 - T_2)}$  (Buoyancy ratio),  $N_T = \frac{AL}{(T_1 - T_2)}$  (Non-dimensional temperature gradient)

$N_c = \frac{BL}{(C_1 - C_2)}$  (Non-dimensional Concentration gradient),  $P = \frac{\mu C_p}{\lambda}$  (Prandtl Number),

$\alpha = \frac{QL^2}{\lambda}$  (Heat source parameter)

The corresponding boundary conditions are

$$u = 0, \theta = 1, C = 1 \text{ on } y = -1$$

$$u = 0, \theta = 0, C = 0 \text{ on } y = +1 \tag{15}$$

### 3. SOLUTION OF THE PROBLEM

The governing equations of flow, heat and mass transfer are coupled non-linear differential equations. Assuming the porosity  $\delta$  to be small we write

$$u = u_0 + \delta u_1 + \delta^2 u_2 + \dots$$

$$\theta = \theta_0 + \delta \theta_1 + \delta^2 \theta_2 + \dots$$

$$C = C_0 + \delta C_1 + \delta^2 C_2 + \dots \tag{16}$$

Substituting the above expansions in the equations (12)-(14) and equating like powers of  $\delta$ , we obtain equations to the zeroth order as

$$\frac{d^2u_0}{dy^2} = \pi \tag{17}$$

$$\frac{d^2\theta_0}{dy^2} - \alpha_1\theta_0 = (P_1N_T)u_0 \tag{18}$$

$$\frac{d^2 C_0}{dy^2} = (ScN_C)u_0 - \frac{ScS_o}{N} \frac{d^2 \theta_0}{dy^2} \quad (19)$$

The equations to the first order are

$$\frac{d^2 u_1}{dy^2} - (M^2 + D^{-1})u_1 = -G(\theta_0 + NC_0) \quad (20)$$

$$\frac{d^2 \theta_1}{dy^2} - \alpha_1 \theta_1 = (P_1 N_T)u_1 \quad (21)$$

$$\frac{d^2 C_1}{dy^2} = (ScN_C)u_1 - \frac{ScS_o}{N} \frac{d^2 \theta_1}{dy^2} \quad (22)$$

The equations to the second order are

$$\frac{d^2 u_2}{dy^2} - (M^2 + D^{-1})u_2 = -G(\theta_1 + NC_1) - \Delta u_0^2 \quad (23)$$

$$\frac{d^2 \theta_2}{dy^2} - \alpha_1 \theta_2 = (P_1 N_T)u_2 \quad (24)$$

$$\frac{d^2 C_2}{dy^2} = (ScN_C)u_2 - \frac{ScS_o}{N} \frac{d^2 \theta_2}{dy^2} \quad (25)$$

The corresponding conditions are

$$u_0(1) = u_0(-1) = 0, \theta_0(+1) = 0, \theta_0(-1) = 1, C_0(+1) = 0, C_0(-1) = 1 \quad (26)$$

$$u_1(1) = u_1(-1) = 0, \theta_1(+1) = 0, \theta_1(-1) = 0, C_1(+1) = 0, C_1(-1) = 0 \quad (27)$$

$$u_2(1) = u_2(-1) = 0, \theta_2(+1) = 0, \theta_2(-1) = 0, C_2(+1) = 0, C_2(-1) = 0 \quad (28)$$

#### 4. NUSSELT NUMBER AND SHERWOOD NUMBER

The rate of heat transfer (Nusselt Number) is given by  $Nu_{y=\pm 1} = \left( \frac{d\theta}{dy} \right)_{y=\pm 1}$

and corresponding expressions are  $Nu_{y=+1} = b_{38} + \delta b_{40} + \delta^2 b_{42}$ ,  $Nu_{y=-1} = b_{39} + \delta b_{41} + \delta^2 b_{43}$

The rate of mass transfer (Sherwood Number) is given by  $Sh_{y=\pm 1} = \left( \frac{dC}{dy} \right)_{y=\pm 1}$  and corresponding expressions are

$$Sh_{y=+1} = b_{44} + \delta b_{46} + \delta^2 b_{48}, \quad Sh_{y=-1} = b_{45} + \delta b_{47} + \delta^2 b_{49}$$

#### Comparison of the results:

- In the heat transfer case (N=0 & N<sub>1</sub> = 0) the results are in good agreement with Devika Rani *et al* (8)

#### 5. DISCUSSION OF THE RESULTS

In this analysis we discuss we effect of thermo diffusion and radiation on Non-Darcy convective heat and mass transfer flow of a viscous electrically conducting fluid through porous media in vertical channel in the presence of heat generating sources. The equation governing the flow heat and mass transfer or solved by employing a regular perturbation with  $\delta$  as a perturbation Parameter.

The axial velocity (u) is shown increases (1-8) for different values G, M, D<sup>-1</sup>,  $\alpha$ , Sc, S<sub>0</sub>, N and N<sub>1</sub> it is found that the axial flow is in the vertically down word direction (fig.1) represents u with Grashof number G. The magnitude of enhances with increasing G>0 and depreciates with |G|. The Maximum of |u| occurs at y=0. The variation of a with M and D<sup>-1</sup> shows that lesser the permeability of porous medium/higher larger force smaller |u| with entire flow region

(fig. 2 &3). From (fig.4), we find that  $|u|$  depreciates with increase heat generating sources. The variation of  $u$  with Schmidt number ( $Sc$ ) shows that lesser molecular diffusivity larger  $|u|$  (fig.5). The flow region increase the Soret parameter  $|S_0|$  leads to depreciation in  $|u|$  on the entire flow region (fig.6) with respect buoyancy force dominate thermal buoyancy force. The magnitude of  $u$  enhances irrespective of the direction of the buoyancy forces (fig.7). From (fig.8) we find that higher the radiative heat flux smaller  $|u|$  in the flow region.

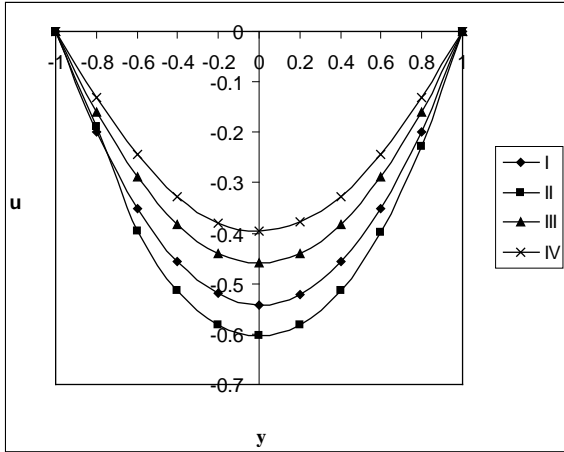


Fig. 1 : Variation of  $u$  with  $G$

	I	II	III	IV
$G$	2	5	-2	-5

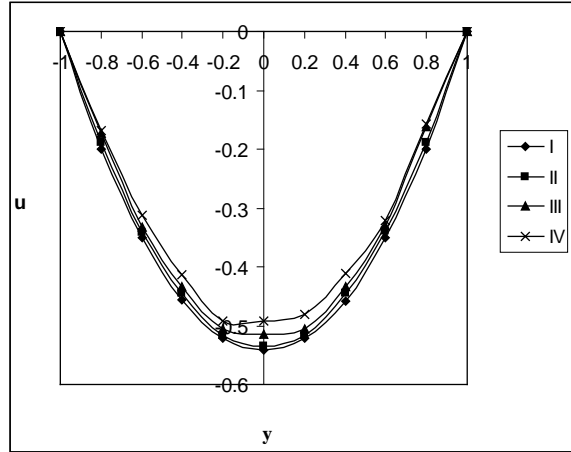


Fig. 2 : Variation of  $u$  with  $M$

	I	II	III	IV
$M$	2	4	6	10

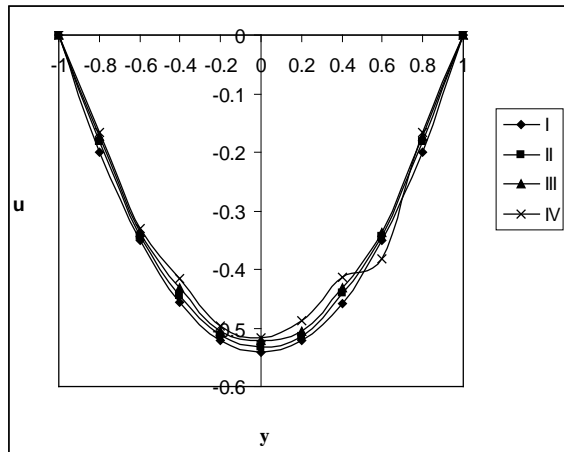


Fig. 3 : Variation of  $u$  with  $D^{-1}$

	I	II	III	IV
$D^{-1}$	2	4	6	10

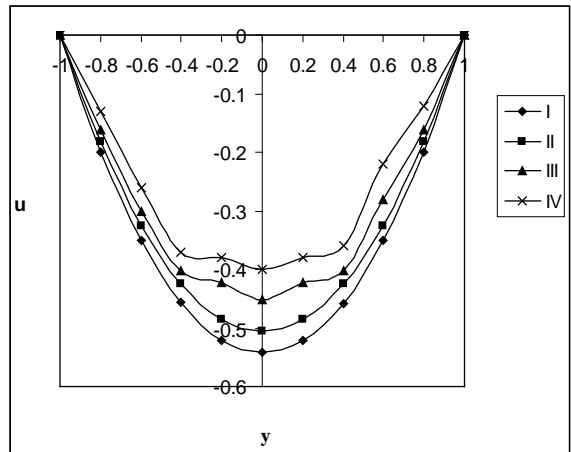


Fig. 4 : Variation of  $u$  with  $\alpha$

	I	II	III	IV
$\alpha$	2	4	6	10

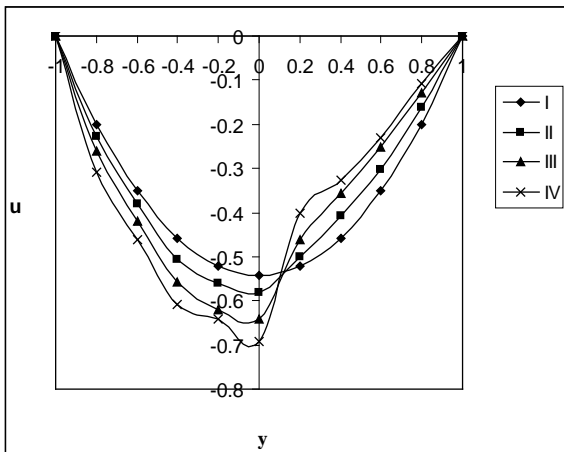


Fig. 5 : Variation of  $u$  with  $Sc$

	I	II	III	IV
$Sc$	0.24	0.6	1.3	2.01

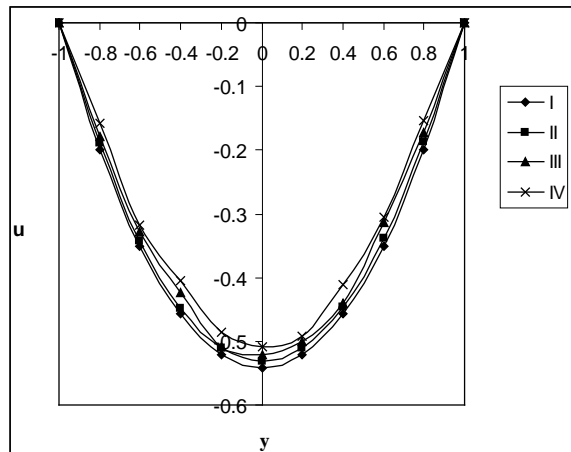


Fig. 6 : Variation of  $u$  with  $S_0$

	I	II	III	IV
$S_0$	0.5	1	-0.5	-1

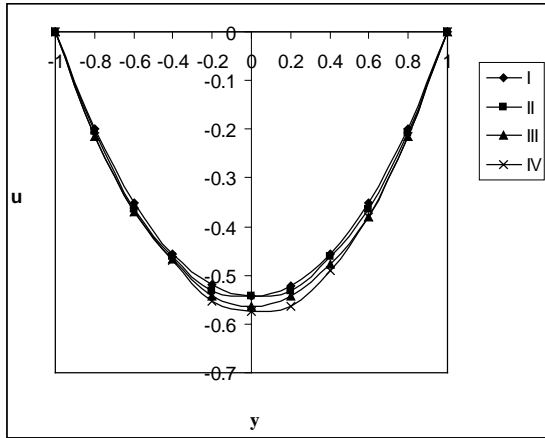


Fig. 7 : Variation of u with N

	I	II	III	IV
N	1	2	-0.5	-0.8

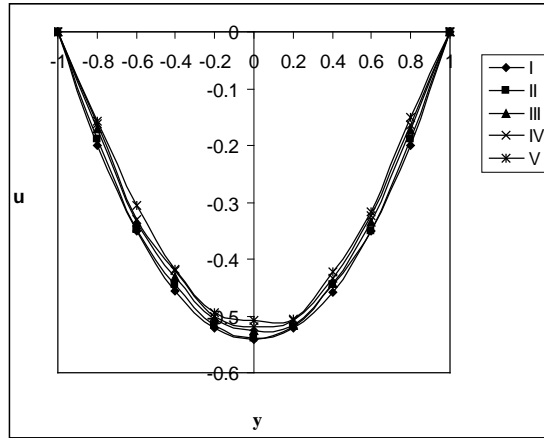


Fig. 8 : Variation of u with N<sub>1</sub>

	I	II	III	IV	V
N <sub>1</sub>	1.5	2.5	5	10	100

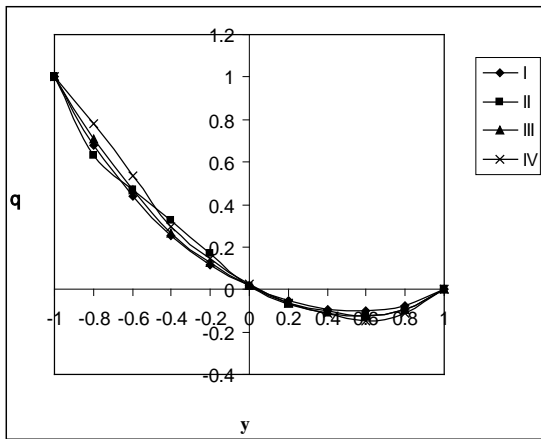


Fig. 9 : Variation of theta with G

	I	II	III	IV
G	2	5	-2	-5

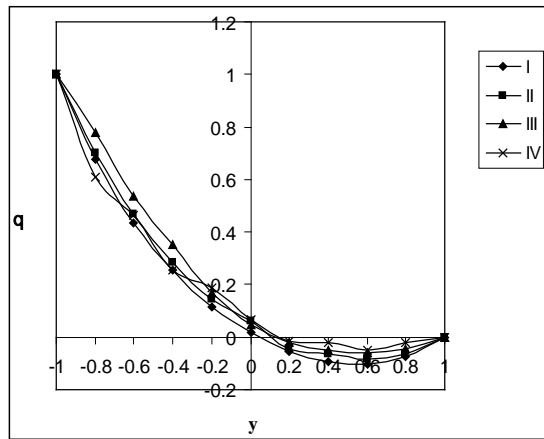


Fig. 10 : Variation of theta with M

	I	II	III	IV
M	2	4	6	10

The non-dimensional temperature ( $\theta$ ) is shown figures (9-16) for different parametric values. We follow the convention that non-dimensional temperature positive or negative according as the actual temperature is greater/lesser than  $T_2$ . Fig. 9 represents  $\theta$  with Grashof number  $G$ . It is found that the actual temperature reduces with increase with  $G > 0$  and enhances with increase in  $G < 0$ . The variation of  $\theta$  with  $M$  and  $D^{-1}$  shows that the lesser permeability of porous medium/higher the Lorentz force, larger the actual temperature in the entire flow region (figs. 10 & 11). An increase in the strength of heat generating source reduces the actual temperature in flow region. The variation of  $\theta$  with  $Sc$  shows that the actual temperature reduces in the left half and enhances in the right half (fig.13). The variation of  $\theta$  the Soret parameter  $S_0$  shows that an increase in  $|S_0|$  enhances the actual temperature in the entire flow region (fig. 14). Then the molecular buoyancy force dominates over the thermal buoyancy force, the actual temperature enhances when the buoyancy forces act in the same direction and for forces act in opposite direction it reduces in the flow region (fig. 15). From (fig. 16) we notice that higher the radiative heat flux smaller the actual temperature in the flow region.

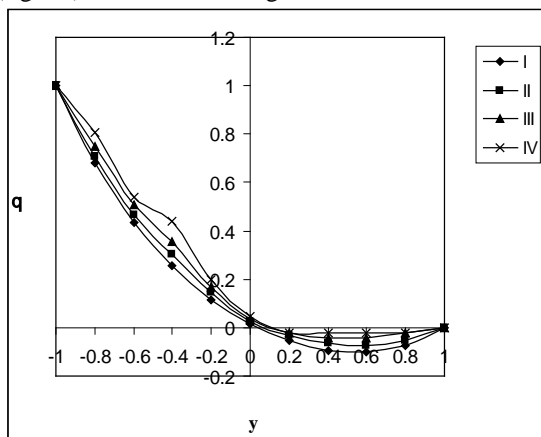


Fig. 11 : Variation of theta with  $D^{-1}$

	I	II	III	IV
$D^{-1}$	2	4	6	10

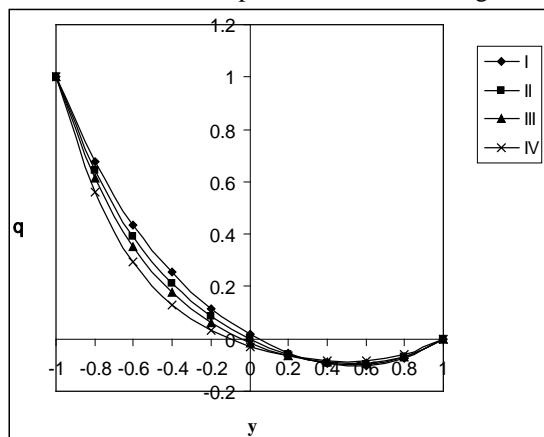


Fig. 12 : Variation of theta with  $\alpha$

	I	II	III	IV
$\alpha$	2	4	6	10

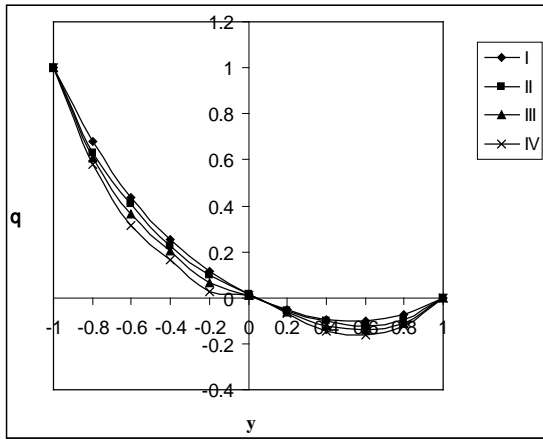


Fig. 13 : Variation of  $\theta$  with  $Sc$   

I	II	III	IV
0.24	0.6	1.3	2.01

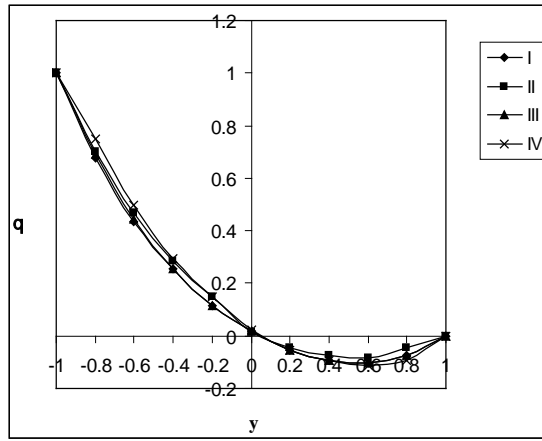


Fig. 14 : Variation of  $\theta$  with  $S_0$   

I	II	III	IV
0.5	1	-0.5	-1

The concentrate distribution (C) is shown in figs (17-24) for different parametric values. We follow the convention that the non-dimensional concentrate is positive or negative according as the actual concentration is greater/lesser than  $C_2$ . Fig.17 represents C with G. It is found that the actual concentration enhances with increase  $G>0$  and for  $G<0$  the actual concentration enhances in the left half and reduces right half of the channel. From (figs 18 & 19), we find that the actual concentration enhances with increase M and  $D^{-1}$ . The variation C with  $\alpha$  shows that the actual concentration depreciates in the left half and enhances in the right half of the (fig. 20), the variation C with Sc shows that lesser the molecular diffusivity larger the actual concentration (fig. 21). The variation of C with Soret parameter  $S_0$  exhibits that the actual concentration enhances with increase  $s_0>0$  and depreciates with  $S_0<0$  (fig. 22). From fig.23, we find that the actual concentration depreciates with  $N>0$  and enhances with  $|N|$  (fig. 23). From (fig. 24) we notice that an increase in the radiation parameter  $N_1$  leads to an enhancement in the actual concentration (fig. 24).

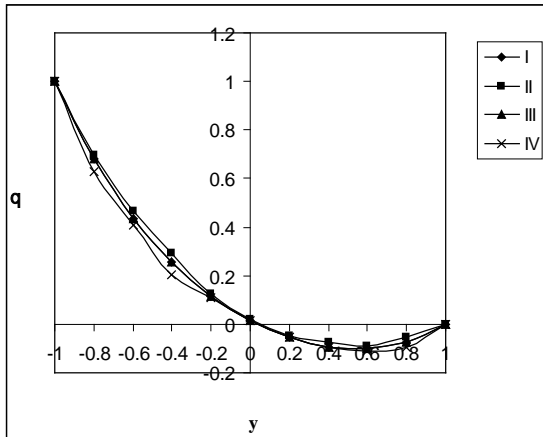


Fig. 15 : Variation of  $\theta$  with  $N$   

I	II	III	IV
1	2	-0.5	-0.8

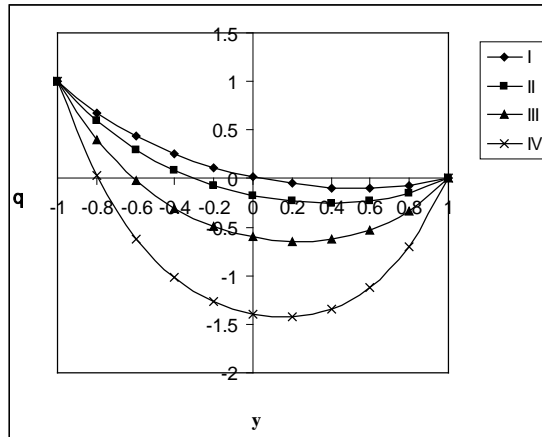


Fig. 16 : Variation of  $\theta$  with  $N_1$   

I	II	III	IV	V
1.5	2.5	5	10	100

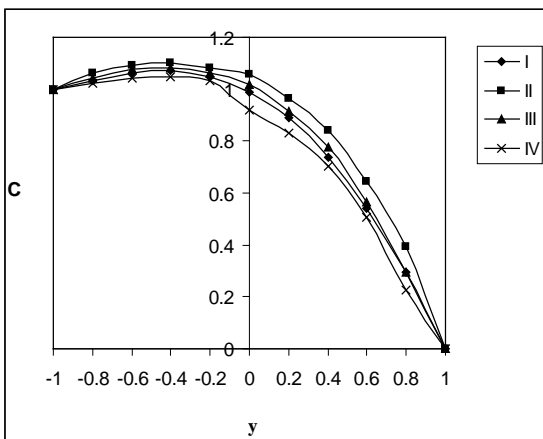


Fig. 17 : Variation of  $C$  with  $G$   

I	II	III	IV
2	5	-2	-5

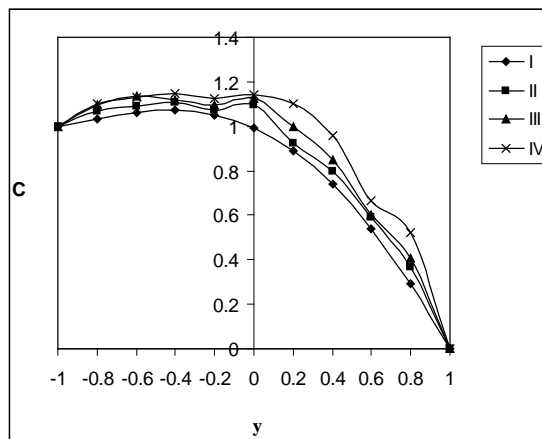


Fig. 18 : Variation of  $C$  with  $M$   

I	II	III	IV
2	4	6	10



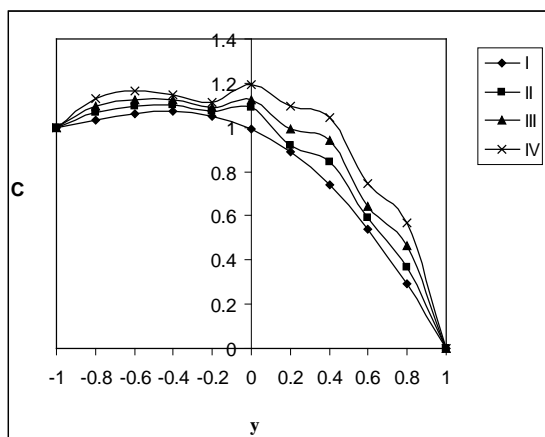


Fig. 19 : Variation of C with  $D^{-1}$

I	II	III	IV	
$D^{-1}$	2	4	6	10

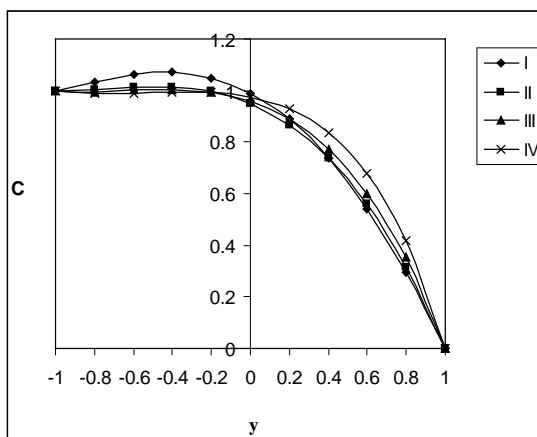


Fig. 20 : Variation of C with  $\alpha$

I	II	III	IV	
$\alpha$	2	4	6	10

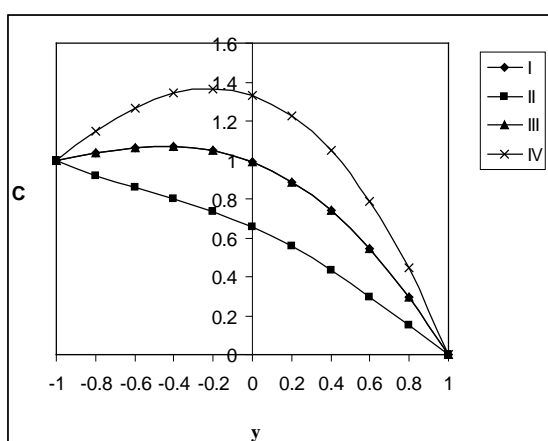


Fig. 21 : Variation of C with  $Sc$

I	II	III	IV	
$Sc$	0.24	0.6	1.3	2.01

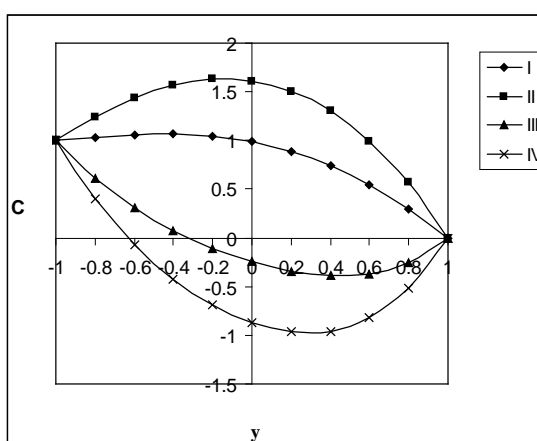


Fig. 22 : Variation of C with  $S_0$

I	II	III	IV	
$S_0$	0.5	1	-0.5	-1

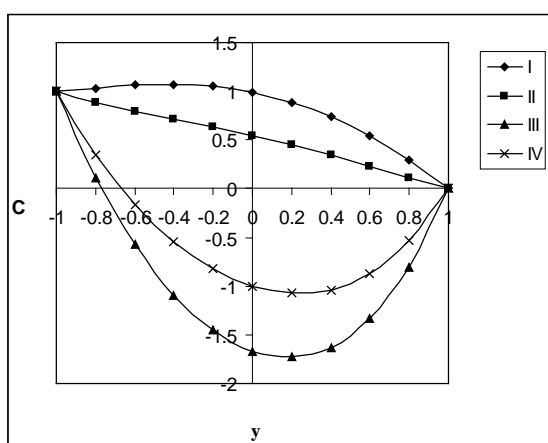


Fig. 23 : Variation of C with  $N$

I	II	III	IV	
$N$	1	2	-0.5	-0.8

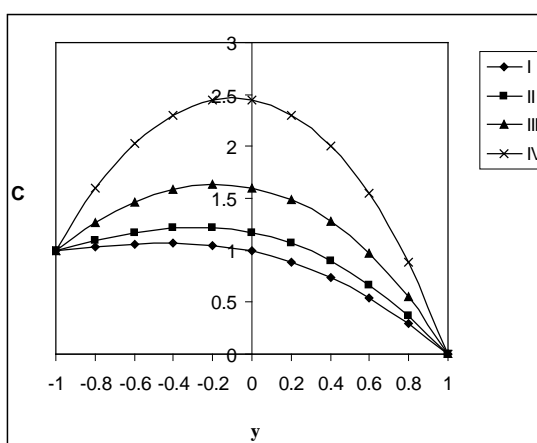


Fig. 24 : Variation of C with  $N_1$

I	II	III	IV	V	
$N_1$	1.5	2.5	5	10	100

The rate of heat transfer (Nusselt number) at  $y=\pm 1$  is shown in (tables 1&4) for different parametric values. It is found that the rate of heat transfer depreciates with increase  $G>0$  and enhance with  $G<0$  at both the walls. An increase in  $M<4$  reduces  $[Nu]$  for  $G>0$  and enhance for  $G<0$  and for higher for  $M>6$ . We notice a reversed effect in the behavior of  $[Nu]$ . The variation  $Nu$  with  $D^{-1}$  shows that lesser the permeability porous media smaller  $[Nu]$  in the heating case and the larger in the cooling case with respect to  $Sc$ . We find that lesser the molecular diffusivity larger  $[Nu]$  for  $G>0$  and smaller for  $G<0$  with respect to Soret parameter  $S_0$ . We find that the rate of heat transfer enhance for  $G>0$  and depreciates with  $G<0$  an increase  $S_0>0$  while for  $S_0<0$  a reversed effect observed in the behavior of  $[Nu]$  (tables 1&3) in the molecular buoyancy force dominates over the thermal buoyancy force the rate of heat transfer enhances for  $G>0$  and reduces for  $G<0$ . When the buoyancy force get in the same direction and for forces act in the opposite direction

|Nu| depreciates in heating case and enhance in the cooling .The variation Nu with radiation parameter N<sub>1</sub> indicates that increase N<sub>1</sub><2.5 depreciates |Nu| at y=+1 and enhance at y=-1 and for further higher N<sub>1</sub>>5 we notice an enhancement in |Nu| for all G. The variation Nu with Eckert number Ec shows that higher the dissipative larger at y=+1 and smaller at y=-1 in the heating case and in the cooling case |Nu| reduces at y=±1 and enhance at y=-1 (tables 2&4).

The rate of mass transfer (Sherwood number) at y=±1 we shown in tables (5-8) for different parametric values. We found that the rate of mass transfer enhance with |G|. An increase in Hartmann number M enhances |Sh| at the both the walls. With respect to D<sup>-1</sup> we find that the rate of mass transfer depreciates with D<sup>-1</sup>≤4 and enhance with D<sup>-1</sup>>6 at y=±1 while at y=-1 |Sh| enhances for G>0 and depreciates for G<0. The variation of Sh with Sc shows that molecular diffusivity larger |sh| at y=+1 and y=-1 lesser |sh|. An increase Soret parameter S<sub>0</sub> results an enhancement |Sh| at the both walls (tables 5&7) when molecular buoyancy force dominates over the thermal buoyancy force the rate of mass transfer depreciates the both walls irrespective of. The direction of the buoyancy forces with respect to N<sub>1</sub>. We find that higher radiative heat flux larger the rate of mass transfer at y=±1. An increase in Ec enhances |Sc| at y=+1 and depreciates at y=-1 (tables 6&8).

**Table – 1**  
Shear stress (τ) at y = +1

G	I	II	III	IV	V	VI	VII	VIII	IX	X	XI
10 <sup>2</sup>	4.16028	-0.36681	-52.16486	4.27910	3.54492	0.93759	2.03209	6.31887	8.11263	-3.74443	-7.69679
3x10 <sup>2</sup>	14.48083	0.89956	-154.49460	14.83730	12.6376	4.81276	8.09626	20.95662	26.33790	-9.23330	-21.09037
-10 <sup>2</sup>	-6.16028	-1.63319	50.16486	-6.27910	-5.54492	-2.93759	-4.03209	-8.31887	-10.11263	1.74443	5.69679
-3x10 <sup>2</sup>	-16.48083	-2.89956	152.49460	-16.83730	-14.63476	-6.81276	-10.09626	-22.95662	-28.33790	7.23330	19.09037
M	2	4	6	2	2	2	2	2	2	2	2
D <sup>-1</sup>	2	2	2	4	8	2	2	2	2	2	2
Sc	1.30	1.30	1.30	1.30	1.30	0.24	0.6	2.01	1.30	1.30	1.30
S <sub>0</sub>	0.5	0.5	0.5	0.5	0.5	0.5	0.5	0.5	1.00	-0.50	-1.00

**Table – 2**  
Shear stress (τ) at y = +1

G	I	II	III	IV	V	VI	VII	VIII	IX
10 <sup>2</sup>	4.16028	2.98988	5.91588	6.26700	3.89990	5.01002	8.20983	2.51893	1.34653
3x10 <sup>2</sup>	14.48083	10.96962	19.74765	20.80101	13.69970	17.03005	26.62948	9.55678	6.03960
-10 <sup>2</sup>	-6.16028	-4.98988	-7.91588	-8.26700	-5.89990	-7.01002	-10.20983	-4.51893	-3.34653
-3x10 <sup>2</sup>	-16.48083	-12.96962	-21.74767	-22.80101	-15.69970	-19.03005	-28.62948	-11.55678	-8.03960
N	1.00	2.00	-0.5	-0.8	1.00	1.00	1.00	1.00	1.00
D <sup>-1</sup>	1.50	1.50	1.50	1.50	2.50	5.00	10.00	1.50	1.50
Ec	0.01	0.01	0.01	0.01	0.01	0.01	0.01	0.03	0.05

**Table – 3**  
Shear stress (τ) at y = -1

G	I	II	III	IV	V	VI	VII	VIII	IX	X	XI
10 <sup>2</sup>	-3.94190	0.10058	51.49493	-4.18420	-3.62687	0.41831	-1.06251	-6.86241	-9.28932	6.75296	12.10039
3x10 <sup>2</sup>	-13.82568	-1.69827	52.48480	-14.55260	-12.88060	-0.74505	-5.18753	-22.58724	-29.86797	18.25888	34.30116
-10 <sup>2</sup>	5.94190	1.89942	-49.49493	6.18420	5.62687	1.58169	3.06251	8.86241	11.28932	-4.75296	-10.10039
-3x10 <sup>2</sup>	15.82568	3.69827	-150.48480	16.55260	14.88060	2.74505	7.18753	24.58724	31.86797	-16.25888	-32.30116
M	2	4	6	2	2	2	2	2	2	2	2
D <sup>-1</sup>	2	2	2	4	8	2	2	2	2	2	2
Sc	1.30	1.30	1.30	1.30	1.30	0.24	0.6	2.01	1.30	1.30	1.30
S <sub>0</sub>	0.5	0.5	0.5	0.5	0.5	0.5	0.5	0.5	1.00	-0.50	-1.00

**Table – 4**  
Shear stress (τ) at y = -1

G	I	II	III	IV	V	VI	VII	VIII	IX
10 <sup>2</sup>	-3.94190	-2.77149	-5.69750	-6.04862	-3.49704	-4.19438	-6.61274	-2.54502	-1.54725
3x10 <sup>2</sup>	-13.82568	-10.31448	-19.09250	-20.14586	-12.49112	-14.58315	-21.83821	-9.63506	-6.64176
-10 <sup>2</sup>	5.94190	4.77149	7.69750	8.04862	5.49704	6.19438	8.61274	4.54502	3.54725
-3x10 <sup>2</sup>	15.82568	12.31448	21.09250	22.14586	14.49112	16.58315	23.8321	11.63506	8.64176
N	1.00	2.00	-0.5	-0.8	1.00	1.00	1.00	1.00	1.00
N <sub>1</sub>	1.50	1.50	1.50	1.50	2.50	5.00	10.00	1.50	1.50
Ec	0.01	0.01	0.01	0.01	0.01	0.01	0.01	0.03	0.05

**Table – 5**  
Nusselt number (Nu) at y = +1

G	I	II	III	IV	V	VI	VII	VIII	IX	X	XI
10 <sup>2</sup>	0.23091	0.21414	0.22317	0.22748	0.22124	0.23021	0.23045	0.23138	0.23177	0.22919	0.22833
3x10 <sup>2</sup>	0.21491	0.17395	0.21660	0.20619	0.19059	0.21282	0.21353	0.21632	0.21749	0.20977	0.20719
-10 <sup>2</sup>	0.24690	0.25433	0.22975	0.24877	0.25190	0.24760	0.24736	0.24643	0.24604	0.24862	0.24948
-3x10 <sup>2</sup>	0.26290	0.29453	0.23632	0.27007	0.28255	0.26500	0.26428	0.26149	0.26032	0.26805	0.27062
M	2	4	6	2	2	2	2	2	2	2	2
D <sup>-1</sup>	2	2	2	4	8	2	2	2	2	2	2
Sc	1.30	1.30	1.30	1.30	1.30	0.24	0.6	2.01	1.30	1.30	1.30
S <sub>0</sub>	0.5	0.5	0.5	0.5	0.5	0.5	0.5	0.5	1.00	-0.50	-1.00

**Table – 6  
Nusselt number (Nu) at y = +1**

G	I	II	III	IV	V	VI	VII	VIII	IX
10 <sup>2</sup>	0.23091	0.23638	0.22271	0.22107	0.75039	1.93026	4.18476	0.14839	0.15719
3x10 <sup>2</sup>	0.21491	0.23132	1.19031	0.18539	0.73775	1.91878	4.17151	0.03866	0.11597
-10 <sup>2</sup>	0.24690	0.24143	0.25510	0.25674	0.76303	1.94174	4.19800	0.25813	0.19841
-3x10 <sup>2</sup>	0.26290	0.24649	0.28750	0.29242	0.77567	1.95322	4.21124	0.36786	0.23963
N	1.00	2.00	-0.5	-0.8	1.00	1.00	1.00	1.00	1.00
D <sup>-1</sup>	1.50	1.50	1.50	1.50	2.50	5.00	10.00	1.50	1.50
Ec	0.01	0.01	0.01	0.01	0.01	0.01	0.01	0.03	0.05

**Table – 7  
Nusselt number (Nu) at y = -1**

G	I	II	III	IV	V	VI	VII	VIII	IX	X	XI
10 <sup>2</sup>	-1.30765	-1.29298	-1.32520	-1.28687	-1.30536	-1.26765	-1.28765	-1.32705	-1.32765	-1.28760	-1.26765
3x10 <sup>2</sup>	-1.26765	-1.26298	-1.29526	-1.26667	-1.22531	-1.24760	-1.26762	-1.280765	-1.29765	-1.26785	-1.24760
-10 <sup>2</sup>	-1.32705	-1.36298	-1.29520	-1.34682	-1.30561	-1.40760	-1.36785	-1.30705	-1.30705	-1.34765	-1.36765
-3x10 <sup>2</sup>	-1.36765	-1.39298	-1.34520	-1.38687	-1.40561	-1.46765	-1.38762	-1.34706	-1.38765	-1.36766	-1.38765
M	2	4	6	2	2	2	2	2	2	2	2
D <sup>-1</sup>	2	2	2	4	8	2	2	2	2	2	2
Sc	1.30	1.30	1.30	1.30	1.30	0.24	0.6	2.01	1.30	1.30	1.30
S <sub>0</sub>	0.5	0.5	0.5	0.5	0.5	0.5	0.5	0.5	1.00	-0.50	-1.00

**Table – 8  
Nusselt number (Nu) at y = -1**

G	I	II	III	IV	V	VI	VII	VIII	IX
10 <sup>2</sup>	-1.30765	-1.32765	-1.30765	-1.28765	-1.69712	-2.75578	-4.94078	-1.27200	-1.24654
3x10 <sup>2</sup>	-1.28765	-1.29765	-1.29765	-1.27760	-1.66712	-2.72578	-4.90078	-1.26206	-1.22654
-10 <sup>2</sup>	-1.32760	-1.34765	-1.34765	-1.36766	-1.70712	-2.78578	-4.99078	-1.29202	-1.34650
-3x10 <sup>2</sup>	-1.34762	-1.32765	-1.36765	-1.308795	-1.72712	-2.82578	-4.52078	-1.32201	-1.36656
N	1.00	2.00	-0.5	-0.8	1.00	1.00	1.00	1.00	1.00
N <sub>1</sub>	1.50	1.50	1.50	1.50	2.50	5.00	10.00	1.50	1.50
Ec	0.01	0.01	0.01	0.01	0.01	0.01	0.01	0.03	0.05

**Table – 9  
Sherwood number (Sh) at y = +1**

G	I	II	III	IV	V	VI	VII	VIII	IX	X	XI
10 <sup>2</sup>	-1.06061	-3.76430	-23.01955	-1.01422	-2.15113	-0.30533	-0.55992	-1.57607	-2.01025	0.76147	1.63390
3x10 <sup>2</sup>	-2.56596	-4.54511	-24.25677	-1.31654	-2.54010	0.23843	-0.42900	-3.13346	3.62257	1.31562	2.14060
-10 <sup>2</sup>	-1.55525	-2.98348	-21.78232	-1.51230	-1.76217	-0.84909	-1.09084	-2.01867	-2.39793	0.20732	1.12721
-3x10 <sup>2</sup>	-2.04989	-2.20266	-20.54510	-1.61018	-1.87320	-1.39285	-1.62175	-2.46127	-2.78561	-0.34682	0.62052
M	2	4	6	2	2	2	2	2	2	2	2
D <sup>-1</sup>	2	2	2	4	8	2	2	2	2	2	2
Sc	1.30	1.30	1.30	1.30	1.30	0.24	0.6	2.01	1.30	1.30	1.30
S <sub>0</sub>	0.5	0.5	0.5	0.5	0.5	0.5	0.5	0.5	1.00	-0.50	-1.00

**Table – 10  
Sherwood number (Sh) at y = +1**

G	I	II	III	IV	V	VI	VII	VIII	IX
10 <sup>2</sup>	-1.06061	-0.41016	3.36666	2.30701	1.74014	2.26479	10.24214	-1.08032	-1.15836
3x10 <sup>2</sup>	-2.56596	-0.04246	4.14881	3.1162	1.25255	9.14617	39.55516	-0.68320	-0.95881
-10 <sup>2</sup>	-1.55525	-0.77786	2.58452	1.50241	-2.73283	-6.61660	-19.07089	-1.64829	-1.95792
-3x10 <sup>2</sup>	-2.04989	-1.14555	1.80237	0.69780	-4.72552	-14.49798	-48.38392	-2.13732	-2.55747
N	1.00	2.00	-0.5	-0.8	1.00	1.00	1.00	1.00	1.00
D <sup>-1</sup>	1.50	1.50	1.50	1.50	2.50	5.00	10.00	1.50	1.50
Ec	0.01	0.01	0.01	0.01	0.01	0.01	0.01	0.03	0.05

## 6. REFERENCES

1. Abdul Sattar, Md. And Alam, Md : Thermal diffusion as well as transprotaion effect on MHD free convection and Mass Transfer flow past an accelerated vertical porous plate, Ind Journal of Pure and Applied Maths. Vol. 24, pp.679-688(199)
2. Ayani, M.B. and Fsfahani, J.H.: The effect of radiation on the natural convection induced by a line heat source. Int. J. Numer. Method, Heat fluid flow (U.K.), 16, 28-45 (2006)
3. Balasubramanyam M, Sudarsan Reddy P, Prasada Rao D.R.V.: Non-Darcy viscous electrically conducting heat and mass transfer flow through a porous medium in a vertical channel in the presence on heat generating sources, Int. J. of Appl. Math and Mech. Vol.6 (15), pp.45-45, (2010).
4. Beckermann C., Visakanta R. and Ramadhyani S.: A numerical study of non-Darcian natural convection in a vertical enclosure filled with a porous medium., Numerical Heat transfer 10, pp.557-570
5. Bharathi, K. : convective Heat and Mass Transfer through a porous medium in channels/pipes with radiation and Soret effects, Ph.D. Thesis , S.K. University, Anantapur, India, (2007).

6. Chamkha A.J. Aly A.M. Mansour M.A. : Unsteady natural convective power-law fluid flow past a vertical plate embedded in a non-Darcian porous medium in the presence of a homogeneous chemical reaction, *Nonlinear Analysis: Modeling and control*, vol.15, No.2, pp.139-154 (2010).
7. P.Cheng : Heat transfer in geothermal systems., *Adv. Heat transfer* 14,1-105(1978).
8. Devika Rani B, Vijaya Bhaskar Reddy P, Prasada Rao D.R.V. : Effect of radiation on Non-Darcy convective Heat Transfer through a Porous medium in a vertical channel, *J. Comp. & Mech. Sci. Vol.2(3)*, pp.483-492 (2011).
9. Jha, B. K. and Singh, A. K.: ,*Astrophys. Space Sci.* vol.173, p.251 (1990).
10. Kafousia.N.G. ,*Astrophys. Space Sci.* vol.173, p.251(1990)
11. Kalidas.N. and Prasad, V: Benard convection in porous media Effects of Darcy and Pransdtl Numbers, *Int. Syms. Convection in porous media, non-Darcy effects, proc.25<sup>th</sup> Nat. Heat Transfer Conf.V.1*, pp.593-604 (1988)
12. Kumar. A., Singh,N.P., Singh,A.K., Kumar,H.: MHD free convection flow of a viscous fluid past a porous vertical plate through non-homogeneous porous medium with radiation and temperature gradient dependent heat source in slip glow regime, *Ultra Sci.Phys.Sci (India)* ,18,39-46(2006)
13. Malasetty.M.S,Gaikwad.S.N: Effect of cross diffusion on double diffusive convection in the presence of horizontal gradient,*Int.Journal Eng.Science*, Vol.40,PP773-787(2002)
14. Poulikakos D., and Bejan, A.: The Departure from Darcy flow in *Nat. Convection in a vertical porous layer*, *physics fluids V.28*,pp.3477-3484 (1985)
15. Prasad, V.and Tuntomo, A.: Inertia Effects on Natural Convection in a vertical porous cavity, *numerical Heat Transfer*, V.11, pp.295-320 (1987)
16. Prasad.V: *Natural convection in porous media*.,Ph.D theisi,S.K.University, Anantapur (1983)
17. Prasad.V, F.A, Kulacki and M.keyhani;" *Natural convection in a porous medium"* *J.Fluid Mech.*150p.89-119(1985).
18. Rashad A.M., Bakier A.Y.: MHD effects on non-Darcy forced convection boundary layer flow past a permeable wedge in a porous medium with uniform heat flux, *Nonlinear Analysis: Modeling and control*, vol.14, No.2, pp.249-261 (2009).
19. D. Tien, C.V. and Hong, J.T.: *Natural convection in porous media under non-Darcian and non-uniform permeability conditions*, hemisphere, Washington.C. (1985)
20. T.L.Tong and E.Subramanian: A boundary layer analysis for natural correction in porous enclosures: use of the Brinkman-extended Darcy model,, *Int.J.Heat Mass Transfer.*28,pp.563-571.
21. Vafai, K., Tien, C.L: *Boundary and Inertia effects on flow and Heat Transfer in Porous Media*, *Int. J. Heat Mass Transfer*, V.24. Pp.195-203 (1981)
22. Vafai, K., Thyagaraju, R.: *Analysis of flow and heat Transfer at the interface region of a porous medium*, *Int. J. Heat Mass Trans.*, V.30pp.1391-1405 (1987)
23. G.Laurait and V.Prasad.: *natural convection in a vertical porous cavity a numerical study of Brinkman extended Darcy formulation.*, *J. Heat Transfer.*pp.295-320(1987).

**Source of support: Nil, Conflict of interest: None Declared**